Chinese Physics B

PAPER

Design of photonic crystal fiber with elliptical air-holes to achieve simultaneous high birefringence and nonlinearity

To cite this article: Min Liu *et al* 2018 *Chinese Phys. B* **27** 014206

View the article online for updates and enhancements.

This content was downloaded from IP address 130.239.20.133 on 09/02/2018 at 20:03

Design of photonic crystal fiber with elliptical air-holes to achieve simultaneous high birefringence and nonlinearity*

Min Liu(刘敏)[1,2,†], Jingyun Hou(侯静云)[1], Xu Yang(杨虚)[1], Bingyue Zhao(赵昺玥)[1], and Ping Shum[3]

[1] College of Communication Engineering, Chongqing University, Chongqing 400044, China
[2] Ministry of Education Key Laboratory of Optoelectronic Technology and Systems, Chongqing University, Chongqing 400044, China
[3] School of Electrical & Electronic Engineering, Nanyang Technological University, Singapore

(Received 22 June 2017; revised manuscript received 18 September 2017; published online 28 November 2017)

A new type of V-shaped photonic crystal fiber with elliptical air-holes is proposed to realize simultaneous high birefringence and nonlinearity at a wavelength of 1.55 μm. The full vector finite element method was adopted to investigate its characteristics, including birefringence, nonlinearity, and dispersion. The PCF exhibited a very high birefringence of 2.89×10^{-2} and very high nonlinear coefficient of 102.69 $W^{-1}\cdot km^{-1}$. In particular, there were two zero-dispersion wavelengths (ZDWs) in the visible (X: 640–720 nm and Y: 730–760 nm) and near-infrared regions (X: 1050–1606 nm and Y: 850–1500 nm). The combination of high birefringence and nonlinearity allowed the PCF to maintain the polarization state and generate a broadband super continuum, with potential applications in nonlinear optics.

Keywords: photonic crystal fiber, birefringence, nonlinearity, zero dispersion

PACS: 42.81.Gs, 42.65.–k, 42.81.–i **DOI:** 10.1088/1674-1056/27/1/014206

1. Introduction

Owing to the design flexibility in the cross section, photonic crystal fibers (PCFs)[1,2] can be used to achieve particular properties, such as high birefringence,[3,4] high nonlinearity,[5] endless single modes,[6] and tailored dispersion.[7] PCFs with high birefringence can be used as polarization maintaining fibers (PMFs) to eliminate the effect of polarization mode dispersion (PMD)[8] or to maintain the state of polarization for the production of broadband supercontinuum (SC).[9,10] Moreover, birefringent PCFs can be applied in optical communication, optical sensing, and coherent optical communication systems. Different methods have been reported to achieve high birefringence through the destruction of symmetry, such as changing the air hole diameters along the two orthogonal directions,[11] removing several air holes in the core,[12] and introducing elliptical holes.[13,14] Large birefringences of the order of 10^{-3}–10^{-2} have been demonstrated for PCFs with elliptical air holes. Issa *et al.*[15] have experimentally realized elliptical air-hole PCFs with birefringence of 1×10^{-4} in 2004. Li *et al.*[16] and Wang *et al.*[17] have demonstrated birefringent PCFs by combining circular and elliptical air holes, and the corresponding birefringences were 1.09×10^{-2} and 2.54×10^{-2}, respectively. However, it is difficult to fabricate PCFs with both circular and elliptical air holes.

Highly birefringent PCFs with nonlinear properties have received growing attention in telecommunication and supercontinuum applications. Lee *et al.*[18] have experimentally demonstrated a PCF with high birefringence of the order of 10^{-3} and a nonlinear coefficient of 31 $W^{-1}\cdot km^{-1}$ for the use of optical code-division multiple access (OCDMA) applications. Moreover, Kudlinski *et al.*[19] have shown that a PCF with a nonlinear coefficient of 31 $W^{-1}\cdot km^{-1}$ and two zero-dispersion wavelengths (ZDWs), exhibited a higher power spectral density than that of one with a ZDW.

It is important to simultaneously obtain a high level of birefringence, large nonlinearity, and ZDWs[20] to generate the broadband supercontinuum. Ademgil *et al.*[21] designed a PCF with a birefringence of 2.65×10^{-2} and nonlinear coefficient of 49 $W^{-1}\cdot km^{-1}$ with two ZDWs. Although Zhang *et al.*[22] have proposed a PCF consisting of a central defect core and cladding with elliptical air holes, that can produce a high nonlinear coefficient of 150 $W^{-1}\cdot km^{-1}$, the birefringence is only 2.5×10^{-3}. Recently, Rashid *et al.*[23] proposed an octagonal photonic crystal fiber (OPCF) to produce a large birefringence of 2.04×10^{-2} with two ZDWs in the telecommunication bands, but its nonlinearity was only 33 $W^{-1}\cdot km^{-1}$.

In this paper, we designed a new type of V-shaped PCF to simultaneously achieve a high birefringence of 2.89×10^{-2} and high nonlinearity of 102.69 $W^{-1}\cdot km^{-1}$ at a wavelength of 1.55 μm, as well as two ZDWs. The proposed PCF was composed of a solid silica core and cladding, with V-shaped alternating large and small elliptical air-holes. By using the full-vector finite element method (FV-FEM) with anisotropic perfectly matched layers (PMLs), the birefringence, nonlinear coefficient and dispersion were investigated.

*Project supported by the National Natural Science Foundation of China (Grant No. 61475029).
†Corresponding author. E-mail: liumin@cqu.edu.cn
© 2018 Chinese Physical Society and IOP Publishing Ltd

2. Structure and theoretical analysis

The cross section of the designed PCF is shown in Fig. 1. To introduce a high birefringence into the PCF, the cladding had a V-shaped design with large and small elliptical air holes to destroy the six-fold symmetry of the PCF. The refractive index of the background silica was obtained by the Sellmeier equation.[24] The air hole distance was Λ. The diameters of the large and small elliptical air holes along the x- and y-axes directions are D_x, D_y, and d_x, d_y, respectively. The ellipticity of the elliptical air holes was defined as $\eta = D_y/D_x = d_y/d_x$.

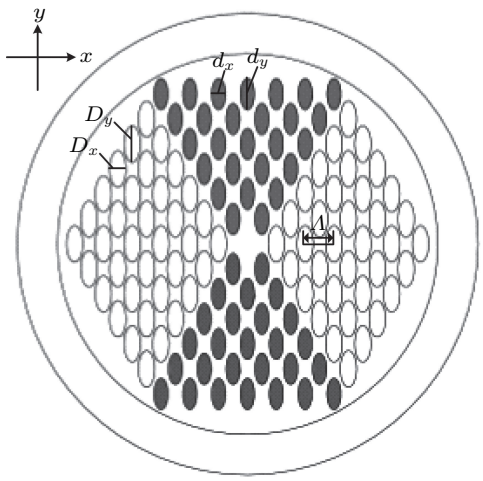

Fig. 1. (color online) Schematic cross-section of the PCF.

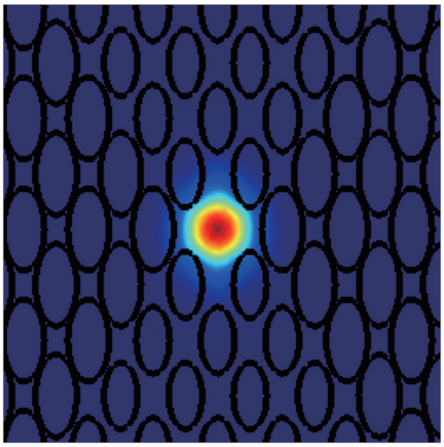

Fig. 2. (color online) Electric field distribution of X for the polarized modes at 1550 nm with $D_x = 0.64\Lambda$, $d_x = 0.52\Lambda$, $\Lambda = 0.8$ μm, and $\eta = 0.5$

The mode analysis was based on the cross section of the PCF structure as the wave propagated in the z direction. Figures 2 and 3 show the fundamental mode field distribution of the PCF at 1550 nm with $D_x = 0.64\Lambda$, $d_x = 0.52\Lambda$, $\Lambda = 0.8$ μm, and $\eta = 0.5$ for the X and Y polarized modes, respectively. The PCF has the characteristics of a single-mode fiber, implying that the mode field energy was fully confined in the core. However, both mode fields tended to be elliptical in the y-axis direction. This is because the air filling ratio in the x-axis direction was greater than that in the y-axis direction, resulting in a reduction of the effective refractive index in the x-axis direction.

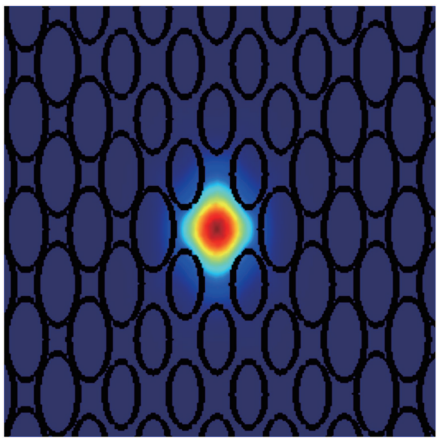

Fig. 3. (color online) Electric field distribution of the Y polarized modes at 1550 nm with $D_x = 0.64\Lambda$, $d_x = 0.52\Lambda$, $\Lambda = 0.8$ μm, and $\eta = 0.5$

The full vectorial finite element method (FEM) is calculated by the following equation, with a magnetic field formulation derived from the Maxwell equation

$$\nabla \times (\varepsilon_\gamma^{-1} \nabla \times H) - K_0^2 \mu_\gamma H = 0, \tag{1}$$

where $\boldsymbol{H}$ is the magnetic field, and ε_γ and μ_γ are the relative dielectric permittivity and magnetic permeability, respectively. K_0 is the wave number in a vacuum, $K_0 = 2\pi/\lambda$, where λ is the operating wavelength. The magnetic field of the modal solution can be expressed as $\boldsymbol{H} = \boldsymbol{h}(x,y)\exp(-\mathrm{j}\beta z)$, where $h(x,y)$ is the field distribution on the transverse plane. The propagation constant β is represented as $\beta = n_{\mathrm{eff}} K_0$. Based on the complex modal effective index, n_{eff}, and the propagation constant, β, the modal birefringence, nonlinearity, and dispersion can be obtained.

The mode birefringence is an important parameter to measure for the polarization performance of the fiber. The modal birefringence is expressed as

$$B = \left|\mathrm{Re}(n_{\mathrm{eff}}^y - n_{\mathrm{eff}}^x)\right|, \tag{2}$$

where n_{eff}^x and n_{eff}^y are the effective refractive indices of two orthogonal polarization fundamental modes, respectively, and Re represents the real part of the effective refractive index.

The nonlinear coefficient $\gamma(\lambda)$ of the PCF can be calculated by

$$\gamma(\lambda) = \frac{2\pi n_2}{\lambda A_{\mathrm{eff}}}, \tag{3}$$

where $n_2 = 3.2 \times 10^{-20}$ m^2·W^{-1} is the nonlinear refractive index of the silica material and A_{eff} is the effective mode area obtained by

$$A_{\mathrm{eff}} = \frac{\left(\iint_\Omega E^2 \mathrm{d}x\mathrm{d}y\right)^2}{\iint_\Omega E^4 \mathrm{d}x\mathrm{d}y}, \tag{4}$$

where E is the transverse component of the electric field propagating inside the fiber and Ω is the cross section of the fiber.

The dispersion or chromatic dispersion of the PCF consists of the material and waveguide dispersions. In general, the waveguide dispersion $D(\lambda)$ depends on the effective refractive index of the fundamental mode and is given by

$$D(\lambda) = -\frac{\lambda}{c}\frac{\partial^2 |\mathrm{Re}(n_{\mathrm{eff}})|}{\partial \lambda^2}, \tag{5}$$

where c is the velocity of the light in vacuum, λ is the wavelength of the light, and $\mathrm{Re}(n_{\mathrm{eff}})$ is the real part of the effective refractive index.

3. Result and discussion

It is important to study the effects of the parameters on the birefringence, nonlinearity, and dispersion of the PCF. The effects of Λ on the birefringence with $D_x = 0.64\Lambda$, $d_x = 0.52\Lambda$, and $\eta = 0.5$ are shown in Fig. 4. The birefringence increases with the wavelength. However it decreased when Λ increased. This is reasonable as a larger Λ can weaken the role of the mode field and the center core. A high birefringence of 2.8911×10^{-2} at 1.55 μm was observed when $\Lambda = 0.8$ μm, $D_x = 0.64\Lambda$, $d_x = 0.52\Lambda$, and $\eta = 0.5$.

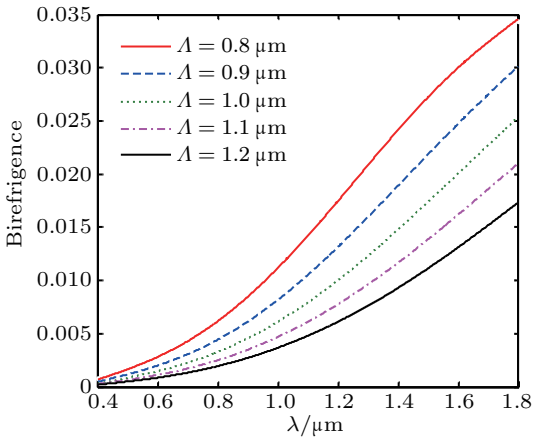

Fig. 4. (color online) Birefringence as a function of wavelength for varying Λ with $D_x = 0.64\Lambda$, $d_x = 0.52\Lambda$, and $\eta = 0.5$.

The ellipticity has a great influence on the birefringence, as illustrated in Fig. 5. Figure 5(a) shows the birefringence as a function of D_x at $\lambda = 1.55$ μm with $d_x = 0.52\Lambda$, $\Lambda = 0.8$ μm, and $\eta = 0.5$. Figure 5(b) presents the birefringence as a function of d_x at $\lambda = 1.55$ μm with $D_x = 0.64\Lambda$, $\Lambda = 0.8$, and $\eta = 0.5$. We observe the opposite change in the birefringence by tuning D_x and d_x. The birefringence increases with D_x, but decreases with increasing d_x. As can be seen from Fig. 5(a), the birefringence is the smallest when $D_x = d_x = 0.52\Lambda$. This is because the diameters of the large and small elliptical air holes along the x- and y-axes directions are the same, implying that the size difference between them is minimal. With increasing D_x, the difference becomes greater inducing a greater index difference between the x- and y-axes as a consequence. Similarly, as shown in Fig. 5(b), when $D_x = d_x = 0.64\Lambda$, the birefringence, i.e., the index difference between x- and y-axes, was minimal. For decreasing d_x, the birefringence increases. We note that although a greater birefringence can be obtained when $d_x = 0.48\Lambda$, the fundamental mode cannot be totally confined in the core. Therefore, to maximize the birefringence, and to ensure a good performance of the structure, the parameters $D_x = 0.64\Lambda$, $d_x = 0.52\Lambda$, and $\eta = 0.5$ are used.

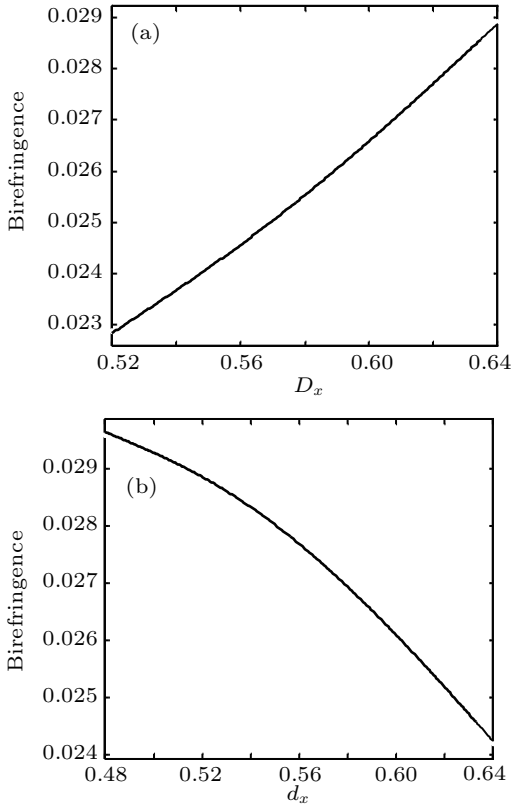

Fig. 5. (a) Dependence of the birefringence on D_x with $d_x = 0.52\Lambda$, $\Lambda = 0.8$, and $\eta = 0.5$ at $\lambda = 1.55$ μm. (b) Dependence of birefringence on d_x with $D_x = 0.64\Lambda$, $\Lambda = 0.8$, and $\eta = 0.5$ at $\lambda = 1.55$ μm

The influence of Λ on the nonlinear coefficient is given in Fig. 6 for the same parameters as Fig. 4. Generally speaking, the nonlinear coefficient decreased when the wavelength and Λ increased. In particular, the PCF with the smallest Λ had the highest nonlinearity at the shorter wavelength region. The main reason for this is that most of the optical energy is limited in the core at the shorter wavelength region, as for the small Λ case. However, parts of the energy will leak into the cladding at the longer wavelength region. The obtained nonlinear coefficients are 78.68 and 77.63 $\mathrm{W^{-1}\cdot km^{-1}}$ for the X-polarized (HE_{11}^{X}) and Y-polarized (HE_{11}^{Y}) modes, respectively, with $\Lambda = 0.8$ μm, $D_x = 0.64\Lambda$, $d_x = 0.52\Lambda$, $\eta = 0.5$, and $\lambda = 1550$ nm. Hence, our PCF achieves high birefringence and nonlinearity at 1550 nm.

Table 1. Birefringence and nonlinearity of the proposed PCF and other PCFs ($\lambda = 1550$ nm).

PCF structure	Birefringence	Nonlinearity/W^{-1}·km^{-1}	Ref.
Hexagonal honeycomb lattice	1.02×10^{-2}	45.7	[11]
V-shape and hexagonal lattice	2.43×10^{-2}	44.38	[25]
Two smaller elliptical holes replace three air-holes	1.53×10^{-2}	42	[12]
Double crescent and hexagonal lattice	4.51×10^{-3}	32.8972	[26]
Elliptical and semi-elliptical air holes	2.54×10^{-2}	54.61	[17]
Elliptical air-holes and rectangular lattice	1.98×10^{-2}	–	[27]
Asymmetric elliptical hole with a central defect hole	3.05×10^{-2}	43.6	[28]
Our proposed PCF	2.89×10^{-2}	78.68	

When the lattice constant was increased to $\Lambda = 1.2$ μm, much higher nonlinear coefficients of 96.651 and 102.69 W^{-1}·km^{-1} in the X and Y polarized modes, respectively, are obtained. We have listed the birefringence and nonlinearities of the proposed PCF and other PCFs designed for polarization-dependent nonlinear applications in Table 1.

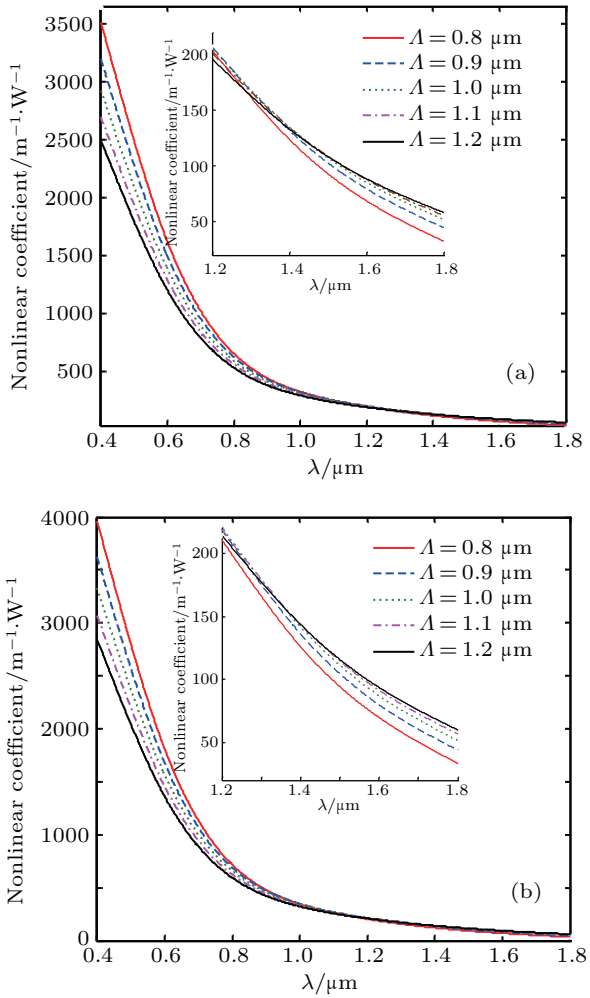

Fig. 6. (color online) Nonlinear coefficient as a function of wavelength for different Λ with $D_x = 0.64\Lambda$, $d_x = 0.52\Lambda$, and $\eta = 0.5$ in (a) X and (b) Y polarized modes.

The dispersion of the PCF is also investigated with the same parameters: $\Lambda = 0.8$ μm, $D_x = 0.64\Lambda$, $d_x = 0.52\Lambda$, and $\eta = 0.5$, and is shown in Fig. 7. There are clearly two ZDWs in the visible and near infrared wavelength regions. As for the X polarized mode, the first ZDW ranges from 640 to 720 nm, and the second ZDW is tuned between 1050 and 1606 nm. As for Y polarized mode, the first ZDW is from 730 to 760 nm, and the second ZDW is between 850 and 1500 nm. Both ZDWs shift towards longer wavelengths (red-shift) with increasing Λ from 0.8 to 1.2 μm. It is observed that zero dispersion is realized at 1550 nm.

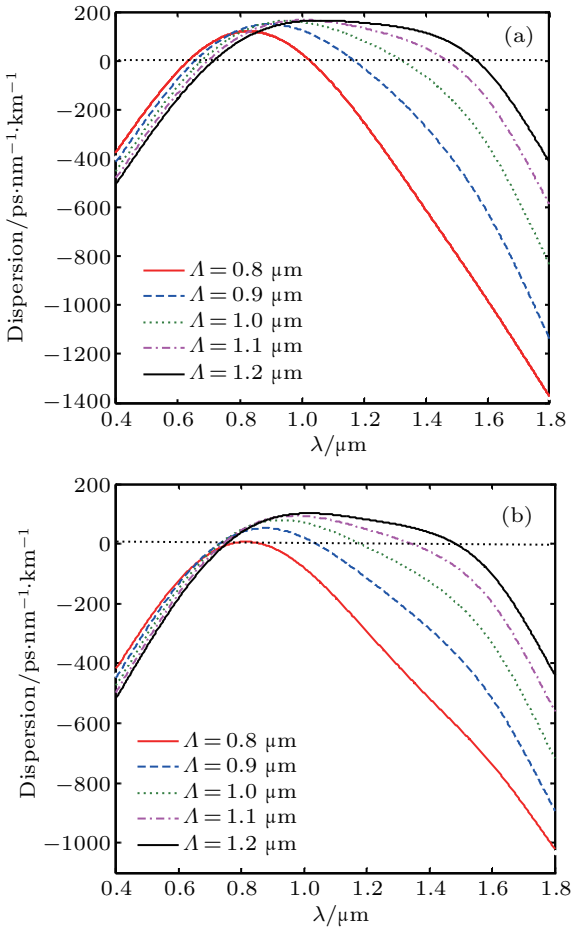

Fig. 7. (color online) Dispersion of (a) X and (b) Y polarized modes for different Λ with $D_x = 0.64\Lambda$, $d_x = 0.52\Lambda$, and η =0.5

Finally, the effects of the air-hole ellipticity on the birefringence and nonlinearity were investigated by fixing $\Lambda = 0.8$ μm, $D_x = 0.64\Lambda$ and, $d_x = 0.52\Lambda$, and the results are shown in Figs. 8 and 9, respectively. It can be seen from Fig. 8 that the birefringence increases with decreasing ellipticity. This can be easily understood, as for a lower ellipticity

the PCF becomes more dissymmetric. In addition, the birefringence increased with the wavelength. In Fig. 9, both decreases in the air-hole ellipticity and wavelength lead to the increase in the nonlinear coefficient.

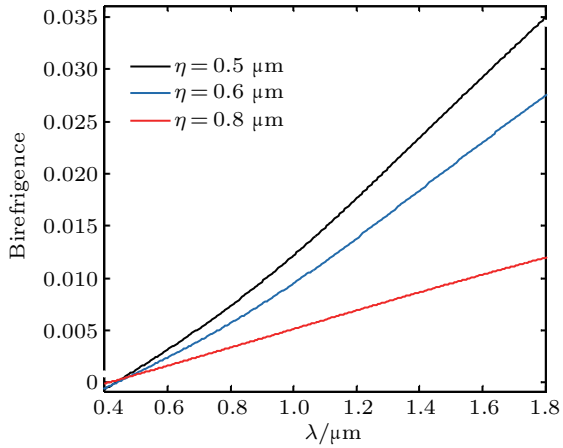

Fig. 8. (color online) Birefringence as a function of wavelength for different η with $D_x = 0.64\Lambda$, $d_x = 0.52\Lambda$, and $\Lambda = 0.8$ μm.

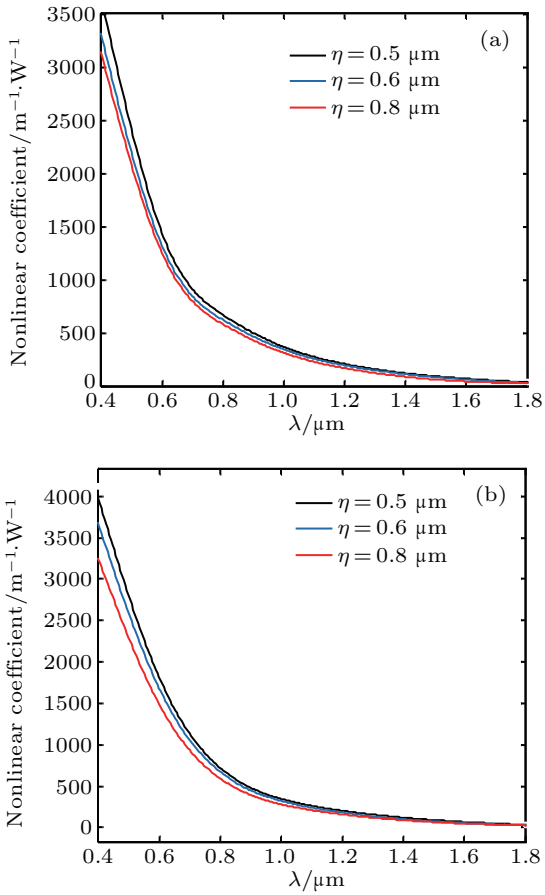

Fig. 9. (color online) Nonlinear coefficient as a function of wavelength for different η with $D_x = 0.64\Lambda$, $d_x = 0.52\Lambda$, and $\Lambda = 0.8$ μm in the (a) X and (b) Y polarized modes.

4. Conclusion

Based on the full-vector finite element method with anisotropic perfect match layers, we designed a PCF that simultaneously obtained a high birefringence of 2.89×10^{-2} and nonlinear coefficient of 78.68 $W^{-1}\cdot km^{-1}$ at a wavelength of 1.55 μm. In addition, two ZWDs occurred in the operation band of the Ti:sapphire oscillator (700 nm–980 nm) and C band. The useful features of simultaneous high birefringence and high nonlinearity, as well as two ZWDs, show potential for nonlinear optics applications, such as supercontinuums, four-wave-mixing, and pulse compression and reshaping.

References

[1] Knight J C, Birks T A, Russell P S J and Atkin D M 1996 *Opt. Lett.* **21** 1547

[2] Cregan R F, Mangan B J, Knight J C, Birks T A, Russell P S J, Roberts P J and Allan D C 1999 *Science* **285** 1537

[3] Kim S E, Kim B H, Lee C G, Lee S, Oh K and Kee C S 2012 *Opt. Express* **20** 1385

[4] Yang T Y, Wang E L, Jiang H M, Hu Z J and Xie K 2015 *Opt. Express* **23** 8329

[5] Wu M, Liu H R and Huang D X 2007 *Study On Optical Communications* **5** 45 (in Chinese)

[6] Gangwar R K, Mishra S S and Singh V K 2014 *Optik* **125** 1641

[7] Zografopoulos D C, Vázquez C, Kriezis E E and Yioultsis T V 2011 *Opt.Express.* **19** 21680

[8] Hasan M R, Anower M S and Hasan M I 2016 *Opt. Engineering* **55** 056107

[9] Hilligsøe K M, Andersen T V, Paulsen H N, Nielsen C K and Mølmer K 2004 *Opt. Express* **12** 1045

[10] Fang L, Zhao J L, Gan X T, Li P and Zhang X J 2010 *Acta Photon. Sin.* **39** 1921

[11] Xu Q, Miao R C and Zhang Y N 2012 *Acta Phys. Sin.* **61** 234210 (in Chinese)

[12] Cao Y, Li R M and Tong Z R 2013 *Acta Phys. Sin.* **62** 084215 (in Chinese)

[13] Hu D J J, Shum P P, Lu C and Ren G B 2009 *Opt. Commun.* **282** 4072

[14] Zhou M H and Huang Y L 2016 *Acta Photon. Sin.* **45** 0306002 (in Chinese)

[15] Issa N A, van Eijkelenborg M A, Fellew M, Cox F, Henry G and Large M C J 2004 *Opt. Lett.* **29** 1336

[16] Li D, Liu M, Jian D, Liao Z Y and He D D 2012 *Chin. J. Lasers* **39** 0405005 (in Chinese)

[17] Wang E L, Jiang H M, Xie K and Zhang X X 2014 *Acta Phys. Sin.* **63** 134210 (in Chinese)

[18] Lee J H, Teh P C, Yusoff Z, Ibsen M, Belardi W, Monro T M and Richardson D J 2002 *IEEE Photon. Techn. Lett.* **14** 876

[19] Kudlinski A, Cumberland B A, Travers J C, Bouwmans G, Quiquempois Y and Mussot A 2008 *AIP Conf. Proc.* **1055** 15

[20] Zhang L 2016 *Ultra-Broadly Tunable Light Sources Based on the Nonlinear Effects in Photonic Crystal Fibers* (Berlin Heidelberg: Springer Theses) pp. 19–39

[21] Ademgil H and Haxha S 2009 *Opt. Commun.* **282** 2831

[22] Zhang Y N, Ren L Y, Gong Y K, Li X H, Wang Zhang Y N, Ren L Y, Gong Y K, Li X H, Wang L R and Sun C D 2010 *Appl. Opt.* **49** 3208

[23] Rashid M M, Anower M S, Hasan M I and Hasan M R2017 *International Conference on Electrical Engineering & Information Communication Techonology*

[24] MalitsonI H 1965 *J. Opt. Soc. Am.* **55** 1205

[25] Li L X, Yu C X, Yuan J H and Wei S 2013 *Asia Communications & Photonics Conference* AF2D.28

[26] Li D M, Zhou G Y, Xia C M, Wang C and Yuan J H 2014 *Chin. Phys. B* **23** 044209

[27] Sheng Y, Lu J, Yao G F and Hu L 2014 *Acta Photon. Sin.* **43** 0106008 (in Chinese)

[28] Yang T Y, Jiang H M, Wang E L and Xie K 2016 *J. Infrared Millim. Waves* **35** 350 (in Chinese)